ChemComm

COMMUNICATION

View Article Online
View Journal | View Issue





Cite this: *Chem. Commun.*, 2022, **58**, 1350

Received 28th October 2021,
Accepted 21st December 2021

DOI: 10.1039/d1cc06049j

rsc.li/chemcomm

# Tumour enzyme affinity mediated peptide molecular crowding for targeted disruption of hyperactivated glucose uptake†

Germain Kwek,[a] Shonya Lingesh,[a] Sayba Zafrin Chowdhury[a] and Bengang Xing *[ab]

**An unconventional environment-responsive molecular crowding *via* specific binding between small molecule peptide inhibitor derivatives and an overexpressed tumour enzyme has been developed. Assemblies of such short peptides selectively localize on tumour surfaces and exhibited unique functions in disrupting hyperactivated glucose uptake, providing novel insights towards strategic tumour treatment.**

Molecular crowding is a natural phenomenon in which biomolecules (such as small lipids, peptides, large structural proteins and polysaccharides) are tightly packed within a limited intracellular space.[1] Despite being in an extremely compact environment, the corresponding concentration and distribution of various biomolecules are nonetheless well-adapted and heterogeneously varied by nature in a well-controlled manner in order to sustain life.[2] Recent studies have highlighted the importance of a dense and complex macromolecular composition to accurately simulate physiological performance[3] in the fields of chemical biology studies,[4] novel drug discoveries[5] and enhanced medical diagnostics.[6]

Intriguingly, there have also been increasing reports of molecular crowding being critical in affecting different characteristics and properties of diseases[7] such as tumours.[8] Recent studies demonstrated that incorporating inert crowder polymers into the extracellular matrix negatively impedes proliferation and hinders the adhesion ability of cancer cells.[9] Moreover, differential responses from cancer and normal cells upon the addition of polymers to mimic mucinous tumour microenvironments have also been investigated. Selective elongation and scattering, an effect commonly known to be a result of reduced proliferation and enhanced migration, was observed to be induced in cancer cells while no major change was observed in normal cells.[10] Nonetheless, the detrimental effects on proliferation and metastasis of cancers and tumours caused by the degree of macromolecular crowding have also been explicitly studied.[11] To date, molecular crowding is commonly achieved through extensive crowding of the extracellular microenvironment with various macromolecular crowder polymers *etc.*[12] Simple, environment-responsive molecular crowding instigated by small molecular based platforms still remain elusive.

Recently, developments in small molecular peptide-based self-assemblies have received tremendous attention and have been well-applied for various disease imaging, detection, and therapies.[13] Particularly, such simple and unique small molecular peptide-based designs can selectively induce environmental responsive molecular crowding systems that predominantly occur at specific subcellular locations[14] and organelles such as the nucleus,[15] mitochondria[16] and Golgi apparatus[17] to cause detrimental effects selectively in diseased areas. However, most of the reported developments mainly focus on reaction-based morphological changes to induce molecular crowding. The extensiveness of the enzymatic activity and saturation of the active site might pose potential drawbacks in complex living systems. On the other hand, simple and direct binding affinity based molecular crowding that can specifically localize at subcellular locations for selective perturbation of cellular activities remains less exploited.[18]

As an attractive therapeutic target in human cancer,[19] furin is a unique membrane-localized proteolytic enzyme[20] in which its aberrant overexpression is an observed characteristic in many malignant tumours.[21] As such, furin activated intracellular self-assemblies of small molecular peptides have been vastly reported for various imaging and therapeutic applications.[22] Therefore, leveraging on the innate enrichment of furin expression in tumours, we propose a simple yet novel tumour enzyme affinity mediated molecular crowding system. Herein, we present an unconventional alternative by exploiting inhibitor-like binding affinities to an enzymatic active site,

[a] *Division of Chemistry and Biological Chemistry, School of Physical & Mathematical Sciences, Nanyang Technological University, 21 Nanyang link, 637371, Singapore. E-mail: bengang@ntu.edu.sg*
[b] *School of Chemical and Biomedical Engineering, Nanyang Technological University, 62 Nanyang Drive, 637459, Singapore*

† Electronic supplementary information (ESI) available. See DOI: 10.1039/d1cc06049j

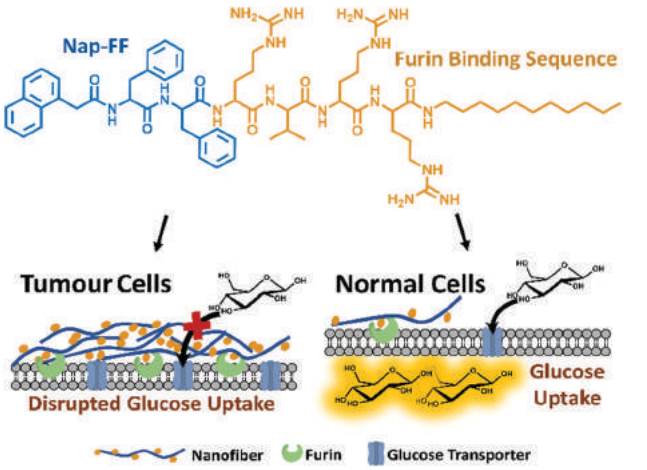


Fig. 1 Molecular structure of the peptidyl furin inhibitor derivative and tumour enzyme affinity mediated molecular crowding for the selective disruption of glucose uptake. The furin binding sequence (yellow) tightly binds to furin on the cellular surface, while Nap-FF (blue) endows the inhibitor derivative with hydrogelating properties.

subsequently bringing about an extensive molecular crowding selectively on the surface of tumour cells to disrupt vital cellular activities (Fig. 1). Typically, a furin-specific peptide sequence (RVRR),[20] which strongly binds to its catalytic active site, was chosen to react with Nap-FF,[23] a commonly used hydrogelating moiety for the purpose of controlled self-assembly in aqueous solutions. To endow potent inhibitor-like properties, the C-terminal was amidated with an 11-carbon alkyl chain.[24] This highly hydrophobic alkyl moiety is also expected to provide substantial interactions for both pericellular membrane anchoring[25] and enhanced driving forces for nanofiber self-assembly.[26]

Upon successful synthesis, the proposed peptidyl furin inhibitor derivative was characterised using HPLC, MS and NMR (Fig. S2–S4, ESI†). The binding affinity of the peptide derivative to the furin enzyme was further examined by determining its inhibition potency ($K_i$ = 3.0 ± 0.1 μM), which is comparable to similar sequences with potent enzyme affinities[24] (Fig. S10, ESI†). Such desired furin binding affinities motivated us to further study the self-assembly of the compound in aqueous solution. To this end, a stock solution of the furin peptide derivative (100 μM) was added dropwise into the buffer. The morphological properties were further investigated with TEM (Fig. 2A). Moreover, higher concentrations of the furin peptide derivative (10 mM) afforded a self-supporting translucent gel (Fig. 2B), clearly elucidating the successful formation of self-assembly in solution. Furthermore, prolonged incubation of the furin peptide derivative in serum or buffer exhibited no obvious degradation even after 48 hours (Fig. S5, ESI†), indicating sufficient stability for subsequent live cell experiments.

We next studied the feasibility of tumour selective molecular crowding in live cells. In this study, human colon carcinoma, HCT116 was selected as the target due to its characteristic overexpression of furin.[27] While a normal colon fibroblast,

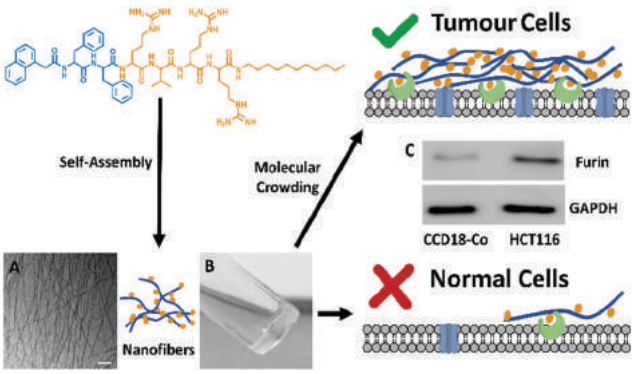


Fig. 2 Nanofiber self-assembly properties of the furin peptide derivative (A) TEM at 100 μM, scale bar: 0.5 μm and (B) translucent gel at 10 mM. Different extents of molecular crowding in tumour and normal cells due to (C) contrasting furin expressions.

CCD18-Co[19] with a properly regulated furin expression was chosen as the negative control. Malignant HCT116 cells were first confirmed to severely overexpress furin compared to CCD18-Co *via* a western blot analysis (Fig. 2C). Upon confirmation of the furin expression in both cell lines, HCT116 and CCD18-Co were each incubated with 100 μM of the furin peptide derivative. Spatial accumulation of the furin peptide derivative in treated cells was examined using Congo red dye, a standard reporter for the indication of self-assembled peptide structures in live cells.[28] The optical microscope images showed an impressive molecular crowding effect with an obvious presence of red gel-like substances covering over the surface of HCT116 (Fig. 3A). As anticipated, the negative control CCD18-Co exhibited minimal gel-like substances on the cellular surface (Fig. 3B). However, limited molecular crowding was unavoidable, most likely due to the innate normal expression of furin in CCD18-Co (Fig. 2C). To rule out the significant contribution of non-specific pericellular membrane anchoring by

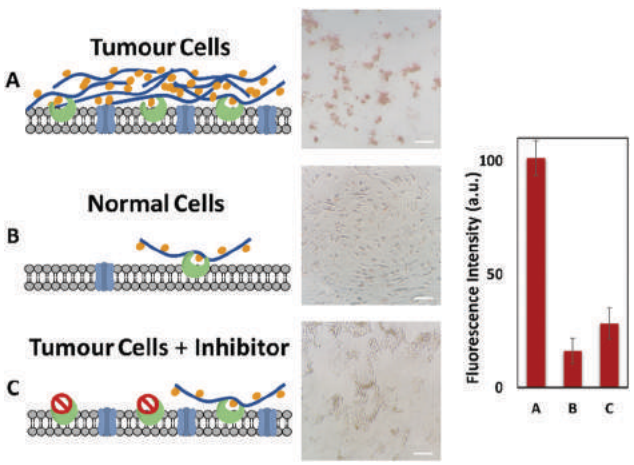


Fig. 3 Optical images of Congo red stained molecular crowding induced on (A) tumour cells, (B) normal cells and (C) tumour cells pre-treated with the furin inhibitor before furin peptide derivative incubation (100 μM), scale bar: 300 μm. Congo red fluorescence intensity in cell samples. ($\lambda_{ex}$ = 488 nm, $\lambda_{em}$ = 614/50 nm).

the 11-carbon alkyl chain in the molecular structure, and clearly elucidate the dependence of enzyme affinity binding to the extensiveness of molecular crowding observed, the HCT116 cells were subsequently pre-incubated with 200 μM of furin inhibitor to extensively block the furin active sites prior to treatment with the furin peptide derivative. The presence of the red gel-like substances was significantly reduced (Fig. 3C), therefore confirming the trivial effect of non-specific pericellular membrane anchoring.

In addition, confocal laser scanning microscope (CLSM) images (Fig. 4) further confirmed the tumour selectivity and spatial accumulation of the pericellular molecular crowding. Significant fluorescence co-localization of Congo red with a membrane tracker was observed in furin overexpressed HCT116 cells, suggesting extensive nanofiber molecular crowding that was localized mainly on the cellular surface. CCD18-Co on the other hand, with a normal furin expression showed relatively weak Congo red fluorescence emission, and therefore a sparse presence of nanofiber molecular crowding even after similar incubation time periods. The successful extensive spatial accumulation of furin peptide nanofibers selectively on the cell membrane of HCT116 encouraged us to further study the possibility of targeted inhibition of vital cellular activities in tumour cells.

The 'Warburg effect' is a hallmark of cancer, whereby hyperactivated glucose utilisation plays a critical role in aggressive tumour growth.[29] This correspondingly demands heightened glucose diffusion across the cellular membrane, facilitated membrane-bound glucose transporters (GLUTs).[30] Particularly, aberrant overexpression of GLUT1 was reported in gastrointestinal carcinomas[31] with the degree of expression demonstrated as a promising prognostic marker for malignant progression in the colon.[32] As such, HCT116 was further confirmed to severely overexpress GLUT1 compared to CCD18-Co *via* immunostaining (Fig. S6, ESI†). Indeed, this peculiarity can be leveraged for effective tumour targeting. A direct approach would be to literally inhibit GLUT mediated glucose entry into tumour cells, resulting in a complete disruption of their glycolytic pathway.[33] However, a specific blockade remains a key challenge as GLUTs are ubiquitously expressed in almost all mammalian cells.[34] As such, we aimed to further study the possibility of selectively disrupting this hyperactivated glucose uptake in tumour cells *via* the tumour specific enzyme affinity mediated molecular crowding we have developed.

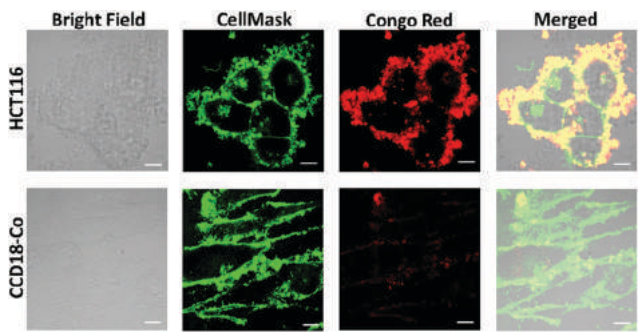


Fig. 4 Confocal images of cells treated with furin peptide derivative (100 μM), subsequently stained with Congo red (0.1 mg mL$^{-1}$) and CellMask membrane tracker (2.5 μg mL$^{-1}$), scale bar: 20 μm. Congo red ($\lambda_{ex}$ = 488 nm, $\lambda_{em}$ = 614/50 nm), Cell Mask ($\lambda_{ex}$ = 640 nm, $\lambda_{em}$ = 670/50 nm).

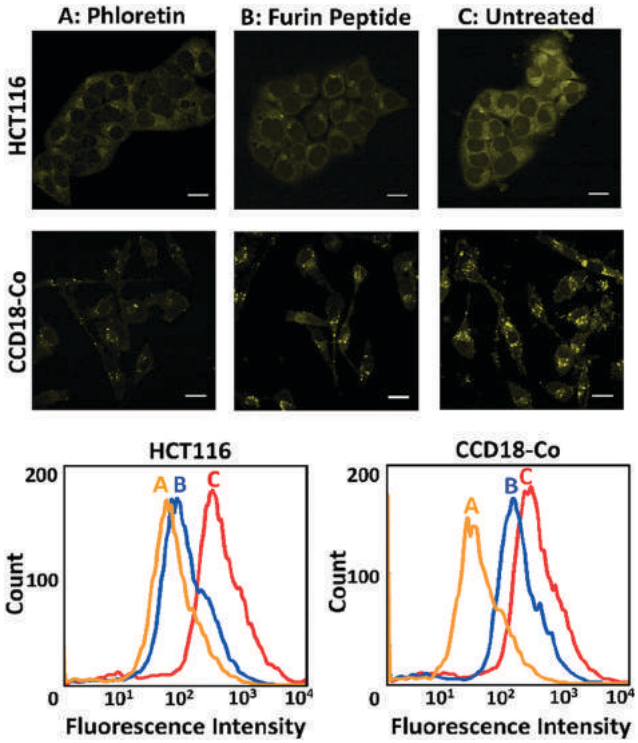


Fig. 5 Confocal images of 2-NBDG (100 μM) uptake upon different treatments, scale bar: 50 μm. Flow cytometric analysis of 2-NBDG fluorescence. 2-NBDG ($\lambda_{ex}$ = 488 nm, $\lambda_{em}$ = 540/50 nm).

[2-(*N*-(7-Nitrobenz-2-oxa-1,3-diazol-4-yl)amino)-2-deoxyglucose] (2-NBDG) is a standard fluorescent D-glucose analogue ideal for evaluating the *in vitro* ability of glucose uptake in mammalian cells.[35] In order to clearly elucidate the tumour selective inhibitory effect of glucose uptake, both HCT116 and CCD18-Co were subjected to different treatments prior to incubation with an equal concentration of 2-NBDG (100 μM). Subsequent CLSM imaging and flow cytometric analysis of 2-NBDG fluorescence were performed to investigate the inhibitory effect on glucose uptake for the corresponding treatment (Fig. 5). Both CLSM imaging and flow cytometric analysis of the relative 2-NBDG fluorescence observed in HCT116 revealed that at the same molar concentration (100 μM), the furin peptide nanofibers could almost inhibit glucose uptake as efficiently as a specific GLUT inhibitor, phloretin.[36] Additionally, a contrast in the molecular crowding extensivity was also observed to selectively inhibit glucose uptake in HCT116 colorectal cancer cells while having a negligible effect on CCD18-Co normal colon cells. Compared to phloretin, which caused a drastic inhibition of the glucose uptake in CCD18-Co as well, our system provides better selectivity by exploiting the versatility of molecular crowding in response to cellular milieu. Furthermore, the experimental concentration of furin peptide

 

derivative (100 μM) was observed to have a limited cytotoxic effect on the cell viabilities of CCD18-Co for up to 48 hours, whereas substantial toxicity was observed in HCT116 (Fig. S7, ESI†). These results clearly show that our system is able to impressively invoke selective inhibition for enhanced tumour targeting with potentially reduced side effects.

In summary, we synthesised a peptidyl furin inhibitor derivative modified with hydrogelating moieties to self-assemble. These assemblies were able to target selectively and accumulate extensively on furin overexpressed tumour cell surfaces due to substantial affinity with furin. Instead of the ordinary exploitation of an erratic proteolytic activity that is characteristic to tumours, we went with the unconventional idea of inducing an extensive molecular crowding *via* enzyme inhibitor binding affinities to disrupt hyperactivated glucose uptake selectively in tumour cells, thus providing novel insights towards new developments in strategic therapy.

The authors acknowledge financial support from the National Natural Science Foundation of China (NSFC) (No. 51929201), Tier 1 RG6/20 and A*Star SERC A1983c0028 (M4070319), and A20E5c0090 from Nanyang Technological University (NTU).

## Conflicts of interest

There are no conflicts to declare.

## Notes and references

1 (*a*) H. G. Hansma, *Origins Life Evol. Biospheres*, 2014, **44**, 307–311; (*b*) T. Lebeaupin, R. Smith and S. Huet, *Nuclear Architecture and Dynamics*, ed. C. Lavelle and J.-M. Victor, Academic Press, Boston, 2018, vol. 2, pp. 209–232; (*c*) A. S. Zembroski and K. K. Buhman, *Lipid Signaling and Metabolism*, ed. J. M. Ntambi, Academic Press, 2020, pp. 131–156.
2 M. A. Mourão, J. B. Hakim and S. Schnell, *Biophys. J.*, 2014, **107**, 2761–2766.
3 D. I. Zeugolis, *Am. J. Physiol.: Cell Physiol.*, 2021, **320**, C842–C849.
4 D. Gnutt and S. Ebbinghaus, *Biol. Chem.*, 2016, **397**, 37–44.
5 N. Puerta Cavanzo, E. Bigaeva, M. Boersema, P. Olinga and R. A. Bank, *Front. Med.*, 2021, **7**, 1092.
6 (*a*) H. Soleimaninejad, M. Z. Chen, X. Lou, T. A. Smith and Y. Hong, *Chem. Commun.*, 2017, **53**, 2874–2877; (*b*) H. Machiyama, T. J. Morikawa, K. Okamoto, T. M. Watanabe and H. Fujita, *Biophys. Physicobiol.*, 2017, **14**, 119–125.
7 J. Jose, A. Anas, B. Jose, A. B. Puthirath, S. Athiyanathil, C. Jasmin, M. R. Anantharaman, S. Nair, C. Subrahmanyam and V. Biju, *ACS Appl. Bio Mater.*, 2019, **2**, 4681–4686.
8 (*a*) R. Damadian, *Science*, 1971, **171**, 1151–1153; (*b*) A. M. DuPre and H. G. Hempling, *J. Cell. Physiol.*, 1978, **97**, 381–396.
9 R. Bascetin, C. Laurent-Issartel, C. Blanc-Fournier, C. Vendrely, S. Kellouche, F. Carreiras, O. Gallet and J. Leroy-Dudal, *Biomaterials*, 2021, **269**, 120610.
10 J. Gonzalez-Molina, J. Mendonça da Silva, B. Fuller and C. Selden, *Sci. Rep.*, 2019, **9**, 8505.
11 (*a*) J.-M. Dubois and B. Rouzaire-Dubois, *Eur. Biophys. J.*, 2004, **33**, 227–232; (*b*) S. Nikolaou and L. M. Machesky, *J. Pathol.*, 2020, **250**, 612–623.
12 P. Benny and M. Raghunath, *J. Tissue Eng.*, 2017, **8**, 2041731417730467.
13 (*a*) F. Gelain, Z. Luo, M. Rioult and S. Zhang, *npj Regener. Med.*, 2021, **6**, 9; (*b*) L. Hu, Y. Li, X. Lin, Y. Huo, H. Zhang and H. Wang, *Angew. Chem., Int. Ed.*, 2021, **60**, 21807–21816; (*c*) X. Xiao, X. Wang, Y. Wang, T. Yu, L. Huang, L. Chen, J. Li, C. Zhang and Y. Zhang, *Chem. – Eur. J.*, 2018, **24**, 2277–2285; (*d*) X. Wang, X. Xiao, B. Zhang, J. Li and Y. Zhang, *Chem. Commun.*, 2019, **55**, 2106–2109; (*e*) G. Kwek, T. C. Do, X. Lu, J. Lin and B. Xing, *ACS Appl. Bio Mater.*, 2021, **4**, 2192–2216; (*f*) H. He, S. Liu, D. Wu and B. Xu, *Angew. Chem., Int. Ed.*, 2020, **59**, 16445–16450; (*g*) Y. Zhong, J. Zhan, G. Xu, Y. Chen, Q. Qin, X. Liao, S. Ma, Z. Yang and Y. Cai, *Angew. Chem., Int. Ed.*, 2021, **60**, 8121–8129; (*h*) Q. Yao, Z. Huang, D. Liu, J. Chen and Y. Gao, *Adv. Mater.*, 2019, **31**, 1804814; (*i*) D. Kalafatovic, M. Nobis, J. Son, K. I. Anderson and R. V. Ulijn, *Biomaterials*, 2016, **98**, 192–202; (*j*) R.-C. Guo, X.-H. Zhang, P.-S. Fan, B.-L. Song, Z.-X. Li, Z.-Y. Duan, Z.-Y. Qiao and H. Wang, *Angew. Chem., Int. Ed*, DOI: 10.1002/anie.202111839.
14 S. Liu and B. Xu, *ACS Omega*, 2020, **5**, 15771–15776.
15 Y. Cai, H. Shen, J. Zhan, M. Lin, L. Dai, C. Ren, Y. Shi, J. Liu, J. Gao and Z. Yang, *J. Am. Chem. Soc.*, 2017, **139**, 2876–2879.
16 (*a*) H. Wang, Z. Feng, Y. Wang, R. Zhou, Z. Yang and B. Xu, *J. Am. Chem. Soc.*, 2016, **138**, 16046–16055; (*b*) H. He, J. Wang, H. Wang, N. Zhou, D. Yang, D. R. Green and B. Xu, *J. Am. Chem. Soc.*, 2018, **140**, 1215–1218; (*c*) H. He, J. Guo, X. Lin and B. Xu, *Angew. Chem., Int. Ed.*, 2020, **59**, 9330–9334.
17 (*a*) C. Fu, J. Zhan, J. Huai, S. Ma, M. Li, G. Chen, M. Chen, Y. Cai and C. Ou, *Nanoscale*, 2020, **12**, 12126–12132; (*b*) R. S. Li, J. Liu, H. Shi, P. P. Hu, Y. Wang, P. F. Gao, J. Wang, M. Jia, H. Li, Y. F. Li, C. Mao, N. Li and C. Z. Huang, *Nano Lett.*, 2021, **21**, 8455–8465.
18 J. Li, K. Shi, Z. F. Sabet, W. Fu, H. Zhou, S. Xu, T. Liu, M. You, M. Cao, M. Xu, X. Cui, B. Hu, Y. Liu and C. Chen, *Sci. Adv.*, 2019, **5**, eaax0937.
19 Y. Yuan, J. Zhang, X. Qi, S. Li, G. Liu, S. Siddhanta, I. Barman, X. Song, M. T. McMahon and J. W. M. Bulte, *Nat. Mater.*, 2019, **18**, 1376–1383.
20 G. Thomas, *Nat. Rev. Mol. Cell Biol.*, 2002, **3**, 753–766.
21 D. E. Bassi, J. Zhang, C. Renner and A. J. Klein-Szanto, *Mol. Carcinog.*, 2017, **56**, 1182–1188.
22 (*a*) X. Li, C. Cao, P. Wei, M. Xu, Z. Liu, L. Liu, Y. Zhong, R. Li, Y. Zhou and T. Yi, *ACS Appl. Mater. Interfaces*, 2019, **11**, 12327–12334; (*b*) J. Chen, Y. Ma, W. Du, T. Dai, Y. Wang, W. Jiang, Y. Wan, Y. Wang, G. Liang and G. Wang, *Adv. Funct. Mater.*, 2020, **30**, 2001566; (*c*) G. Liang, H. Ren and J. Rao, *Nat. Chem.*, 2010, **2**, 54–60.
23 X. Du, J. Zhou and B. Xu, *Chem. – Asian J.*, 2014, **9**, 1446–1472.
24 A. Cameron, J. Appel, R. A. Houghten and I. Lindberg, *Int. J. Biol. Chem.*, 2000, **275**, 36741–36749.
25 (*a*) J. Mu, F. Liu, M. S. Rajab, M. Shi, S. Li, C. Goh, L. Lu, Q.-H. Xu, B. Liu, L. G. Ng and B. Xing, *Angew. Chem., Int. Ed.*, 2014, **53**, 14357–14362; (*b*) C. Zhang, L.-H. Liu, W.-X. Qiu, Y.-H. Zhang, W. Song, L. Zhang, S.-B. Wang and X.-Z. Zhang, *Small*, 2018, **14**, 1703321.
26 (*a*) A. Tanaka, Y. Fukuoka, Y. Morimoto, T. Honjo, D. Koda, M. Goto and T. Maruyama, *J. Am. Chem. Soc.*, 2015, **137**, 770–775; (*b*) J. D. Hartgerink, E. Beniash and S. I. Stupp, *Science*, 2001, **294**, 1684–1688.
27 X. Hu, Z. Hai, C. Wu, W. Zhan and G. Liang, *Anal. Chem.*, 2021, **93**, 1636–1642.
28 (*a*) G. Liang, K. Xu, L. Li, L. Wang, Y. Kuang, Z. Yang and B. Xu, *Chem. Commun.*, 2007, 4096–4098; (*b*) Y. Kuang, J. Shi, J. Li, D. Yuan, K. A. Alberti, Q. Xu and B. Xu, *Angew. Chem., Int. Ed.*, 2014, **53**, 8104–8107.
29 (*a*) C. Liu, Y. Jin and Z. Fan, *Front. Oncol.*, 2021, 11; (*b*) M. V. Liberti and J. W. Locasale, *Trends Biochem. Sci.*, 2016, **41**, 211–218.
30 A. M. Navale and A. N. Paranjape, *Biophys. Rev.*, 2016, **8**, 5–9.
31 Y.-M. Shen, G. Arbman, B. Olsson and X.-F. Sun, *Int. J. Biol. Markers*, 2011, **26**, 166–172.
32 R. S. Haber, A. Rathan, K. R. Weiser, A. Pritsker, S. H. Itzkowitz, C. Bodian, G. Slater, A. Weiss and D. E. Burstein, *Cancer*, 1998, **83**, 34–40.
33 M. Pliszka and L. Szablewski, *Cancers*, 2021, **13**, 4184.
34 Y. Shi, S. Liu, S. Ahmad and Q. Gao, *Curr. Top. Med. Chem.*, 2018, **18**, 454–466.
35 C. Zou, Y. Wang and Z. Shen, *J. Biochem. Biophys. Methods*, 2005, **64**, 207–215.
36 A. Sasaki, K. Nagatomo, K. Ono, T. Yamamoto, Y. Otsuka, T. Teshima and K. Yamada, *Hum. Cell*, 2016, **29**, 37–45.